Journal of Food Composition and Analysis 136 (2024) 106826

Contents lists available at ScienceDirect

Journal of Food Composition and Analysis

journal homepage: www.elsevier.com/locate/jfca

Artificial intelligence tools and concepts give access to authenticity and quality information in Brazilian olive oil volatilome

Nathália S. Brilhante [a], Humberto R. Bizzo [a,b,*], Andrea Caratti [c], Simone Squara [c], Chiara Cordero [c,**]

[a] Universidade Federal do Rio de Janeiro, Avenida Athos da Silveira Ramos, 149, Rio de Janeiro, RJ 21945-970, Brazil
[b] Embrapa Agroindústria de Alimentos, Avenida das Américas, 29501, Rio de Janeiro, RJ 23020-470, Brazil
[c] University of Turin, Dipartimento di Scienza e Tecnologia del Farmaco, Via Pietro Giuria, 11, Torino, TO 10125, Italy

ARTICLE INFO

Keywords:
Brazilian extra virgin olive oil
Volatile compounds
Comprehensive two-dimensional gas chromatography
Aroma blueprint
Authenticity markers
Cultivar markers
Geographic markers

ABSTRACT

Brazil is the world's second largest importer of olive oil and stared to produce its own oil quite recently in two distinct geographic areas. The production is still very small, and studies regarding oil composition are scarce. Determination of discriminant differences are useful to support appeals regarding origin indication and to detect fraud and adulteration with oils from other countries. In this work the Brazilian extra virgin olive oils (EVOOs) volatilome is explored by Artificial Intelligence (AI) tools developed on multiple headspace solid-phase microextraction (MHS-SPME) combined with comprehensive 2D gas chromatography-mass spectrometry and flame ionization detection (GC×GC-MS/FID) data. Using MHS-SPME, external standard calibration, and FID predicted relative response factors (RRF), the accurate quantification of 51 informative volatile compounds was carried out and the odorants responsible for key-positive sensory attributes were used to generate distinctive aroma blueprints aligned with the AI smelling based on sensomics. As authenticity and origin assessment decision-making tool, augmented visualization by computer vision was applied on volatilome 2D fingerprints. By this approach, extra-virgin olive oil samples (n=35), from two olive cultivars (Arbequina and Koroneiki) harvested in the main producing regions in Brazil (Rio Grande do Sul and Serra da Mantiqueira) in 2021 and 2022, were effectively discriminated and mislabeled products regarding their geographical origin were, for the first time, promptly identified.

1. Introduction

Olive oil is a typical food from the Mediterranean region, and is mainly composed of triglycerides (from 97 % to 99 % by weight). The predominant fatty acid in the triglycerides is oleic (C18:1), related to the high nutritional value of the oil. In lower amounts, linolenic (C18:3), linoleic (C18:2), and some saturated fatty acids, such as stearic (C18:0), and palmitic (C16:0) acids are also present. Terpenic acids, mono and diglycerides, free fatty acids, tocopherols, phenolic compounds, sterols, chlorophyll, carotenoids, and volatile compounds are found in minor amounts as a complex mixture of nonpolar, polar, and amphiphilic substances (Mariotti and Peri, 2014).

Within the complex fraction of volatile compounds, several potent odorants with low odor threshold (OT) are responsible for the unique aroma of olive oils (Neugebauer et al., 2020). Extra virgin olive oil (EVOO) has a complex aroma that is related to the genetics of the olive tree (cultivar), the pedoclimatic conditions where trees are grown, the olive maturation stage, and the extraction process applied. The main volatile compounds responsible for the desired green aroma in the oil are produced from the oxidation of linoleic and linolenic fatty acids through the lipoxygenase pathway (LOX), a series of enzymatic chain reactions that occurs during the senescence of the fruit and processing. The main fraction of volatiles produced from LOX are linear unsaturated and saturated alcohols, aldehydes, and esters with six carbons (Olias et al., 1993; Kalua et al., 2007; Kotsiou and Tasioula-Margari, 2015). Not only compounds from LOX are found in EVOOs, but also those related to fatty acid autooxidation. These non-enzymatic reactions result in the formation of hydroperoxide degradation products such as (*E*)-2-heptenal, (*E*)-2-octenal, (*E*)-2-decenal, pentanal, hexanal, heptanal, octanal, nonanal, acetic acid, butanoic acid and hexanoic acid, which are mainly

* Corresponding author at: Universidade Federal do Rio de Janeiro, Avenida Athos da Silveira Ramos, 149, Rio de Janeiro, RJ 21945-970, Brazil.
** Corresponding author.
E-mail addresses: humberto.bizzo@embrapa.br (H.R. Bizzo), chiara.cordero@unito.it (C. Cordero).

https://doi.org/10.1016/j.jfca.2024.106826
Received 31 July 2024; Received in revised form 29 September 2024; Accepted 3 October 2024
Available online 9 October 2024

related to rancid aroma (Morales et al., 1997; Luna et al., 2006; Neugebauer et al., 2020). Mass spectrometry has been successfully used for the identification of more than a hundred volatile compounds in the oil, after separation by gas chromatography (Stilo et al., 2021, 2023).

The world's production of olive oil was 2.7 million tons in the 2022/2023 crop year. The main producers of olive oil in the world are the countries of the European Union with 1.5 million tons in the same crop. Spain, Greece, Italy, and Portugal have the largest production. Due to climate change, during the last years, the production of olive oil in the main countries has been affected. In 2021, Spain produced 1.5 million tons of olive oil and in the next crop, the production decreased to 780,000 tons. At the same time, countries that are not known as olive oil producers (e.g., Brazil, China, and Australia) started and increased their production (International Olive Oil Council - (IOC, 2022).

In this context, Brazil is the second largest importer of olive oil in the world (100,340 tons in 2022) but, despite the high consumption, the growth of olives in the country and, therefore, the extraction of the oil, are quite recent and small in comparison to the size of the domestic market. In 2022, only 503 tons of extra virgin olive oil were produced in Brazil, 0.24 % of the total amount imported in the same year (International Olive Oil Council - (IOC, 2022); (Brazilian Agricultural Research Corporation – Embrapa, 2023). The main EVOO producing regions in Brazil are the state of Rio Grande do Sul (RS) and Serra da Mantiqueira (MA), which corresponds to the states of Minas Gerais, São Paulo, and Rio de Janeiro. The Arbequina (AR) and Koroneiki (KO) cultivars are the most produced in the country (Filoda et al., 2021).

Another important aspect is that edible oils are the most adulterated foods in the world, and olive oil is no exception. It is estimated that between 75 % and 80 % of extra virgin olive oils (EVOOs) sold in the United States are adulterated, and that EVOOs fraud in Italy is an industry worth around 16 billion euros (Sudhakar et al., 2023).

Olive oils volatilome encrypts information regarding the quality of olives (e.g., botanical origin, harvest region, ripening stage) and of oils (e.g., presence of positive aroma attributes, perceivable defects) representing a fraction of analytical interest in qualification, authentication, and certification processes. In this perspective, due to the high chemical dimensionality (i.e., number of chemical classes and series of homologues represented) of EVOOs volatilome, comprehensive two-dimensional gas chromatography (GC×GC) offers many interesting opportunities especially in case of accurate quantification of marker volatiles in presence of co-eluting compounds. Accurate quantification is the primary choice in quality assessment over large time-frame studies enabling a reliable benchmarking of samples against reference products [i.e., *identitation* (Stilo et al., 2021)]. The main advantages of this technique rely on the improved separation efficiency (*i.e.*, peak capacity n or separation measure S) that is the product of the two chromatographic dimensions, and higher method sensitivity achieved by band-compression in space or in time depending on the type of modulation applied (Stilo et al., 2021, 2021a). Due to these characteristics, parallel detection by mass spectrometry (MS) and flame ionization detector (FID), does not suffer of sensitivity drop enabling the exploitation of the FID response factors (RFs) quantification in a large range of concentrations (Stilo et al., 2021b). GC×GC has therefore been successfully applied in the characterization of complex volatile fractions, such in food volatilomics (Nicolotti et al., 2013; Magagna et al., 2017; Magagna et al., 2017; Uekane et al., 2017; Lukić et al., 2019) and in quantitative volatilomics (Stilo et al., 2021c).

With the use of GC×GC techniques, a large amount of data is generated; the use of dedicated data processing algorithms, most of them developed within the domain of Artificial Intelligence (AI) concepts and tools, allows effective exploration of the higher-level information while also providing analysts with prompt and reliable decision-making tools (Caratti et al., 2024). Recently, sensomics conceptualized an AI smelling capable of predicting key-aroma features of food without using human olfaction (Nicolotti et al., 2019). The concept allows prediction of the aroma blueprint of samples based on the peculiar distribution of food key-aroma compounds through their dose over-threshold (*i.e.*, odor activity value, OAV) (Dunkel et al., 2014; Nicolotti et al., 2019; Granvogl and Schieberle, 2022). Interestingly, if a quantitative volatilomics approach is performed, the 2D chromatographic patterns can also be approached with the new AI concept of augmented visualization (Caratti et al., 2023; Cordero et al., 2010; Reichenbach et al., 2009; Schmarr et al., 2010; Schmarr and Bernhardt, 2010; Stilo et al., 2021c). By computer vision, a kind of AI tool, chromatographic traces can be compared, after registration and re-alignment, to visually identify deviations from a reference or highlight marker patterns diagnostic of a specific sample's quality/property.

Regarding Brazilian olive oils, just a few studies explored the volatilome to identify reliable and robust markers of authenticity, identity, and quality. Available data relate to cultivars signatures from olives harvested in Minas Gerais and in the southern region of Brazil (Zago et al., 2019; Carvalho et al., 2020; da Costa et al., 2020; Brilhante et al., 2022; Lima et al., 2023; Stilo et al., 2023). In particular, one study identified potential markers for Koroneiki, Arbequina, Grapollo, and Arbosana EVOOs although the samples' representativeness (n=12) and the lack of accurate quantitative data limits the applicability of these results (Lima et al., 2023).

A first attempt to create a database for quality benchmarking of Brazilian oils was by us (Stilo et al. 2023). In that study, we analyzed 28 commercial samples available on the Brazilian market after 2020 harvest using quantitative volatilomics and compared them to a larger selection of Italian high-quality EVOOs (n=111) identifying country of origin markers and delineating a distinctive aroma signature.

Considering these points, the present study aimed to evaluate the metabolome of volatile compounds of EVOOs from the two main cultivars produced in Brazil (Koroneiki and Arbequina), from the two producing regions of the country (Serra da Mantiqueira and Rio Grande do Sul) during the crops of 2021 and 2022 to discriminate these EVOOs according to their production region and cultivar. To achieve these objectives, advanced AI tools and concepts were applied to fully exploit the information encrypted in the olive oil volatilome while also collecting quantitative data to build a reference database for Brazilian oils quality benchmarking. The set of samples (n=35) investigated covers cultivar-specific signatures (Koroneiki and Arbequina), geographical tracers (Serra da Mantiqueira and Rio Grande do Sul, Brazil), and harvest year impact (crops 2021 and 2022).

2. Material and methods

2.1. Sampling

Thirty-five commercial samples of EVOOs from two crops (2021 and 2022), two geographical areas, Rio Grande do Sul (RS) and Serra da Mantiqueira (MA), and from 2 cultivars (Koroneiki and Arbequina) were acquired at the beginning of each crop. Samples, consisting of 500 mL of olive oil from the same production batch, were kept in their original dark green or amber glass bottles, and stored in a freezer (-20 °C) until analysis. Classification according to EU quality standards, IOC references, and Brazilian protocols was performed at Embrapa's ISO 17025 accredited laboratory (Brasil. Diário Oficial da União, 2012; Brasil. Diário Oficial da União, 2018; The European Commission, 2016). All samples were classified as "extra-virgin" based on their composition and sensory quality profile. The samples were named according to their cultivar, harvest year, and production region, the list of samples together with the acronyms adopted in this study is available in Supplementary Table 1.

2.2. Chemicals

The solvents cyclohexane and dibutyl phthalate (purity: 99 %) and the standards of n-alkanes (from C_9 to C_{25}), used for linear retention indices (I^T) calibration, and methyl 2-octynoate, used as Internal

Standard (ISTD), were from Merck (Milan, Italy).

The key aroma compounds and potent odorants used for external calibration (*E*)-2-nonenal (CAS 18829–56–6), (*E*)-2-octenal (CAS 2548–87–0), heptanal (CAS 111–70–6), (*E,E*)-2,4-hexadienal (CAS 142–83–6), (*E*)-2-hexenal (CAS 6728–26–3), (*Z*)-3-hexen-1-ol (CAS 928–96–1), hexanal (CAS 66–25–1), 1-hexanol (CAS 111–27–3), (*E*)-2-pentenal (CAS 1576–87–0), (*E*)-2-penten-1-ol (CAS 1576–96–1), (*Z*)-2-penten-1-ol (CAS 1576–95–0), 1-penten-3-ol (CAS 616–25–1), 1-pentanol (CAS 71–41–0), and 2-pentanol (CAS 6032–29–7) were all from Sigma Aldrich (Milan, Italy).

2.3. Standard solutions and calibration curves

Quantification of volatile compounds was performed by multiple headspace solid-phase microextraction (MHS-SPME) sampling according to a previously validated procedure (Stilo et al., 2021b) as follows:

Table 1
List of 51 target compounds with their experimental ^{1}D I^{T} and corresponding literature value (Lit. I^{T}), FID predicted relative response factors (RRF), and MHS-SPME decay constant (β) used for quantification purposes. The concentration range of each compound in samples as well as their odor threshold (OT), when available, are presented in ng/g.

Compound Name	Exp. IT	Lit. IT	ID criterion	RRF	β	Odor quality	OT (ng/g)	Concentration range in samples (ng/g)	
								Min.	Máx.
1-Hexanol	1343	1348	a	1	0.77	Fruity, banana, soft	400 ǂ	145.12	5859.18
α-Pinene	1013	1017	b	0.82	0.92	Herbal, woody	274 *	30.34	200.74
p-Xylene	1123	1128	b	0.86	0.86	-	-	<LOQ	63.92
m-Xylene	1130	1140	b	0.75	0.85	-	-	10.29	142.14
Hexanoic acid	1829	1839	b	1.28	0.9	-	-	21.5	266.10
Heptanoic acid	1936	1946	b	1.19	0.91	-	-	10.84	242.34
Decane	998	1000	a	0.78	0.88	-	-	nd	141.04
Toluene	1028	1036	b	1.18	0.95	-	-	57.05	328.57
Phenol	1999	2005	b	1.42	0.91	-	-	59.97	374.22
Pentanoic acid	1722	1734	b	1.1	0.69	-	-	10.32	130.66
Pentanal	971	957	b	0.78	0.82	-	-	210.87	2596.57
Octane‡	-	800	a	0.96	0.93	-	-	nd	67.13
Octanal	1284	1289	b	1.13	0.88	Citrus-like, fatty	140 $	24.82	147.61
Hexyl acetate	1269	1275	b	1.04	0.65	Fruity	200 $	78.44	532.03
Hexanal	1075	1069	a	0.99	0.81	Green-apple, grass	300 $	767.83	4018.75
Heptanal	1179	1181	a	1.12	0.89	Citrus-like, fatty	500 $	20.39	82.08
2-Methylfuran‡	-	855	b	0.86	0.83	-	-	33.97	274.42
Ethylbenzene	1116	1122	b	1.65	0.82	-	-	<LOQ	67.12
3-Methylbutanal	912	911	b	1.1	0.78	Sweet, fruity, malty	5.4 ǂ	11.29	162.50
2-Methylbutanal	908	908	b	1.1	0.74	Sweet, malty	34 $	11.84	242.12
Benzaldehyde	1511	1524	b	0.95	0.92	Almond, burnt sugar	60 *	41.81	170.49
6-Methyl-5-hepten−2-one	1330	1339	b	0.98	0.89	-	-	20.84	309.62
5-Ethyl-2(5 H)-furanone	1744	1757	b	1.41	0.85	-	-	10.72	267.56
(*Z*)-3-Hexenal	1136	1133	b	1.08	0.65	Green, grassy	1.7 $	47.09	7749.33
(*E*)-3-Hexenal	1131	1127	b	1.08	0.64	Artichoke, green, flowers	3.0 ǂ	23.9	923.59
(Z)-3-Hexen-1-ol	1373	1380	a	1.04	0.74	Banana, fresh, grass	1100 *	581.81	9770.32
3,4-Diethyl-1,5-hexadiene (meso)	964	944	b	0.8	0.71	-	-	30.45	134.11
3,4-Diethyl−1,5-hexadiene (RS/SR)	957	936	b	0.81	0.71	-	-	33.79	141.3
(*E*)-2-Pentenal)	1120	1131	a	1.16	0.63	Pungent, apple-like	300 ǂ	92.06	327.40
(Z)-2-Penten-1-ol)	1302	1306	a	1.1	0.61	Green, almond	250 *	291.18	983.51
(*E*)-2-Penten-1-ol)	1310	1313	a	1.1	0.63	Mushroom, earthy	250 *	47.19	131.48
2-Pentanol	1105	1095	a	1.06	0.84	Musty, fermented	380 *	<LOQ	168.89
(*E*)-2-Octenal)	1422	1430	a	0.98	0.88	Fatty, nutty	120 $	15.72	41.45
(*E*)-2-Nonenal)	1528	1534	a	0.95	0.87	Fatty, green, soapy	140 $	<LOQ	45.94
(*Z*)-2-Hexenal	1194	1193	b	1.08	0.59	Fruity	-	58.11	954.60
(*E*)-2-Hexenal)	1213	1216	a	1.08	0.62	Bitter almond, green, fruity	320 $	1857.40	>LOQ
(*E,E*)-2,4-Heptadienal	1455	1461	b	1.06	0.89	Fatty, green, oily	30 $	25.94	102.49
1-Octene‡	-	827	b	0.8	0.8	-	-	9.17	68.76
1-Octanol	1546	1553	b	0.93	0.93	Nut, mushroom	27 *	<LOQ	57.26
1-Penten-3-ol	1151	1157	a	1.1	0.63	Pungent, butter	400 ǂ	317.29	1578.82
1-Pentanol	1240	1240	a	1.06	0.72	Sweet, pungent	470 ǂ	14.47	211.28
3-Methyl-1-butanol	1198	1211	b	1.06	0.65	-	-	16.02	413.57
(*Z*)-3-Hexenyl acetate	1313	1317	b	1.16	0.87	Green	200 ǂ	218.39	3065.17
(*E,Z*)-3,7-Decadiene‡	1071	**	b	0.8	0.83	-	-	64.04	332.12
(*E,E*)-3,7-Decadiene‡	1079	**	b	0.8	0.85	-	-	92.41	792.46
(*E,E*)-2,4-Hexadienal)	1393	1397	a	1.12	0.74	Green	270 *	191.50	1754.29
(*E*)-β-Ocimene	1244	1233	b	0.82	0.91	-	-	9.23	245.46
(*E*)-2-Hexen-1-ol	1395	1398	b	1.04	0.76	Green, grass	5000 ǂ	42.24	9401.67
(*E*)-2-Heptenal	1317	1320	b	1.02	0.85	Green, fatty	1200 $	20.44	111.35
(5*Z*)-3-Ethyl-1,5-octadiene	1008	1006	b	0.8	0.76	-	-	128.27	602.84
(5*E*)-3-Ethyl-1,5-octadiene	1021	1032	b	0.8	0.79	-	-	216.16	955.77

$ Neugebauer et al. (2020)
* Stilo et al. (2021d)
ǂ Luna et al. (2006)
** Not found in literature
‡ Tentative identification
Identification criterion: "a" for analytes confirmed by authentic standards and "b" for those that matched spectral similarity and I^{T} tolerance
Compounds highlighted in bold were quantified by external calibration (further information available in Supplementary Table 2)

quantification of potent odorants in EVOOs by external calibration (14 selected compounds reported in Supplementary Table 2 and highlighted in Table 1 in bold) and quantification of an extended list of marker volatiles (n=52) by FID using predicted relative response factors (RRFs) based on combustion enthalpies and molecular formula (Cachet et al., 2016).

Standard stock solutions of potent odorants were prepared at a concentration of 10 g/L in cyclohexane. The reference working solution (RWS) was prepared by mixing a suitable amount of each standard stock solution to achieve the concentration of 0.200 g/L of each compound using dibutyl phthalate as solvent.

Calibration solutions (CS) were prepared by diluting appropriate amounts of RWS in dibutyl phthalate to reach concentrations of 5, 10, 15, 20, 25, 30, 50, 100, 150, 200, 250, 300, 350, and 400 mg/L. Five microliters of each CS were analyzed by MHS-SPME to build calibration curves to reach absolute amounts of 25, 50, 75, 100, 125, 150, 250, 500, 750, 1000, 1250, 1500, 1750, and 2000 ng. Further information about the procedure is available in the Supplementary Figure 1.

Methyl 2-octynoate (ISTD working solution) was prepared at a concentration of 0.100 g/L in dibutyl phthalate for standard-in-fiber preloading. All prepared solutions were stored at −18°C in sealed vials.

2.4. Multiple headspace solid phase microextraction (MHS-SPME) and quantification of volatile compounds

Volatile compounds were extracted by HS-SPME with a divinylbenzene/carboxen/polydimethylsiloxane (DVB/CAR/PDMS) fiber of 50/30 μm thickness and 2 cm length from Merck-Supelco (Bellefonte, PA, USA). The SPME fiber was conditioned before use as recommended by the manufacturer (Brilhante et al., 2022; Stilo et al., 2021b, 2023).

Methyl 2-octynoate was used as ISTD for response normalization and quality control. ISTD was preloaded onto the SPME fiber by sampling 5.0 μL of a 0.100 g/L solution placed into a headspace vial of 20 mL. ISTD preloading was done by exposing the fiber to the headspace at a temperature of 40°C for 5 min (Stilo et al., 2021b).

Sampling was performed on 0.100 ± 0.005 g of olive oil placed into 20 mL headspace vials kept at 40°C for 60 min under constant agitation. After extraction, the fiber was thermally desorbed into the GC×GC system injector port in split-flow mode (1:5), with an injector temperature of 250°C and a desorption time of 5 min (Stilo et al., 2021b).

MHS-SPME was performed following the conditions described previously. Ten consecutive extractions were carried out for a selection of oil samples and 4–6 for the calibration curve solutions, so that an almost exhaustive extraction of the analytes of interest was achieved and the exponential decay function estimated with greater accuracy. The potent odorants subjected to external calibration together with their odor qualities, odor thresholds (OT) in oil, experimental I^T, regression function parameters including calibration range, and determination coefficients (R^2) are reported in Supplementary Table 2.

The quantification of the 14 potent odorants in the samples was made by external calibration. For the other compounds identified, whenever possible, the quantification was performed by using relative response factors (Cachet et al., 2016; Stilo et al., 2021b).

2.5. GC×GC-MS/FID: Instrument configuration and conditions

Samples were analyzed with a system consisting of an MPS-2 autosampler (Gerstel, Mülheim a/d Ruhr, Germany) installed on a GC×GC system equipped with a reverse-inject differential-flow modulator (Agilent Technologies, Little Falls, DE, USA). The gas chromatograph used was an Agilent 7890B coupled to an Agilent 5977B high-efficiency source (HES) mass spectrometric detector operated in electronic ionization mode at 70 eV for identification. The transfer line temperature was set at 280°C, the ion source at 230°C and quadrupole temperature at 150°C. The scanning range was adjusted between 45 and 240 *m/z*, (acquisition frequency of 30 Hz). For quantification, parallel detection was performed by a fast FID with a base temperature of 280°C, H_2 flow of 40 mL/min, air flow of 350 mL/min, and sampling frequency of 200 Hz (Stilo et al., 2021b).

The column configuration used was: first dimension (^{1}D) HeavyWax (100 % polyethylene glycol - PEG; 20 m × 0.18 mm × 0.18 μm) coupled with a second dimension (^{2}D) DB17 column (50 % phenyl-methylpolysiloxane; 1.8 m × 0.18 mm × 0.18 μm). The connection between the ^{2}D column and the deactivated silica capillaries for the MS (0.5 m × 0.1 mm) and FID (1.1 m × 0.18 mm) for parallel detection was by a three-way non-purged capillary microfluidic splitter (all the supplies were from Agilent Technologies). The resulting split ratio was 70:30 (FID/MS) and the dimensions of the bleeding capillary (6.06 m × 0.1 mm) of deactivated fused silica installed in the modulator plate were chosen according to a previously validated flow calculator (Giardina et al., 2018). The carrier gas was helium at a flow rate of 0.4 mL/min along the ^{1}D column and 10 mL/min along the ^{2}D column. The oven temperature program was set: from 40°C (2.29 min) to 240°C (11 min) at 3.06 °C/min. The modulation period (P_M) was 3 s and the pulsed time was 150 ms (Stilo et al., 2021b).

Compounds were identified by comparison of their mass spectra with those from NIST library, and by their linear retention indices (van Den Dool and Dec. Kratz, 1963) compared to literature data (Adams, 2007; Babushok et al., 2011).

2.6. Computer vision

Computer vision (CV) was applied by generating cumulative class images from the 2D spectra of samples of different cultivars (Arbequina and Koroneiki – Class *cultivar*) and production regions (Rio Grande do Sul and Serra da Mantiqueira – Classes *region*). The approach was used to promptly highlight compositional differences in samples' volatilome and connect them with samples' class characteristics (Caratti et al., 2023; Stilo et al., 2021c).

The workflow used to perform these comparisons was conceptualized by Caratti and co-workers (2023) and further validated for its effectiveness in different applications [e.g., butter volatilome, hazelnut spoilage, etc. (Stilo et al., 2021c; Caratti et al., 2023)].

In this study, CV was performed using GC Image® software according to the following steps:

- Build a cumulative image with samples belonging to a specific Class. In particular, cumulative images were built for EVOOs from Arbequina cultivar, EVOOs from Koroneiki cultivar, EVOOs from Rio Grande do Sul region (RS), and EVOOs from Mantiqueira region (MA);
- Create a *feature template* with reliable peaks and peak-regions specific of a Class of samples. To do this, the smart template configuration included retention times search windows in ^{1}D and ^{2}D (^1t_R; ^2t_R), and MS spectral similarity between reference and analyzed spectra with a direct match factor threshold (DMF – NIST similarity algorithm)> 700 as optimized in previous studies (Stilo et al., 2021, 2021b);
- Apply the feature template created at step-2 on single 2D chromatograms or class image chromatograms to effectively register and re-align patterns before fusion or before comparative visualization;
- Perform comparative visualization between Cumulative Class images of samples with different characteristics via overlaid comparative visualization rendered as a diffuse grayscale ratio to achieve augmented visualization by CV.

2.7. Data treatment and statistical analyses

GC×GC data were processed using GC Image® software version 2021r3 (GC Image, LLC, Lincoln NE, USA). Statistical analyses and chemometrics were carried out by using XLSTAT software (Lumivero, Denver CO, USA). Principal Component Analysis was conducted on both normalized responses for all UT features and accurate amounts of

quantified compounds to highlight natural sample clusters within the sample set. Data was mean centered before PCA analysis. To identify discriminant markers between sample classes, Partial Least Squares Discriminant analysis (PLS-DA) was applied. Discriminant analytes were selected within those with a Variable Importance on the Projections (VIPs) score above 1. For PLS-DA modelling, the training set was composed by all samples while the validation was by randomly selecting a 30 % of samples from the data set. Up to 10 reiterations were applied. For both unsupervised and supervised analysis all replicates per sample were computed (Brereton, 2009).

3. Results and discussion

3.1. The use of MHS-SPME followed by GC×GC-MS/FID for identification and quantification of volatile compounds in EVOOs

EVOO volatilome encrypts information on many key-quality variables *e.g.*, cultivar, geographical origin, cultivation methodologies, oxidation level, and aroma profile (Brilhante et al., 2022; da Costa et al., 2020; Lima et al., 2023; Stilo et al., 2021b, 2023). Using MHS-SPME followed by GC×GC-MS/FID, it was possible to consistently monitor 115 reliable peaks (including targeted and untargeted features), 77 of them identified using linear retention indices (I^Ts) and EI-MS spectral similarity (threshold > 900). Quantification of 51 target volatiles was achieved via MHS-SPME, external standard calibration and FID predicted RRFs (Cachet et al., 2016; Stilo et al., 2021b). The list of the quantified compounds is reported in Table 1 along with information on type of identification, accurate amount in the sample, odor quality, and OT in oil.

From identification and quantification, a database was built and a workflow was established to diagnose markers for authentication according to production region and cultivar: (1) based on the quantification of the target volatile compounds present in Brazilian EVOO samples; partial least squares-discriminant analysis (PLS-DA) and principal component analysis (PCA) were performed to understand if a natural sample clustering according to production region (MA and RS) and cultivar (AR and KO) was possible; (2) CV on Cumulative Class images was further explored to achieve full validation of this prompt tool for authenticity evaluation (Caratti et al., 2023). CV results, in addition to providing immediate visual comparison, also reinforce the results previously obtained in step 1 and allow the use of untargeted compounds in the analysis to find extra discriminant markers; (3) application of Artificial Intelligence smelling machine concept to determine the aroma blueprint in samples from different cultivars (Neugebauer et al., 2020; Stilo et al., 2021b). This step was applied only for cultivar discrimination since is expected that EVOOs produced from different cultivars have distinct sensorial profiles. This workflow provides consistent information to distinguish EVOOs samples according to cultivar and production region and also allows the identification of erroneous allegations regarding cultivar and origin. The comparisons performed are further discussed in the next items.

3.2. Production region volatilome signatures

In Fig. 1A is shown the PCA loadings plot for Arbequina samples produced in 2021 and 2022, colors correspond to production regions and ellipses are set to 95 % of confidence level. Considering this set of samples and their natural clustering according to the production region, two cumulative images were prepared, each consisting of 4 samples. These cumulative images were used for CV by means of comparative visualization rendered as a grayscale fuzzy ratio (Fig. 1B). Arbequina samples from the MA region have higher relative amounts of alcohols and acetic acid (brighter part), while samples of the same cultivar from RS show higher amounts of aldehydes (darker part).

The same procedure was applied to the Koroneiki samples (Fig. 1C and D). To perform these analyses, the sample coded as KO22_MA1 was removed, and this will be discussed further ahead. The PCA showed that there is not a good separation between samples of Koroneiki cultivar

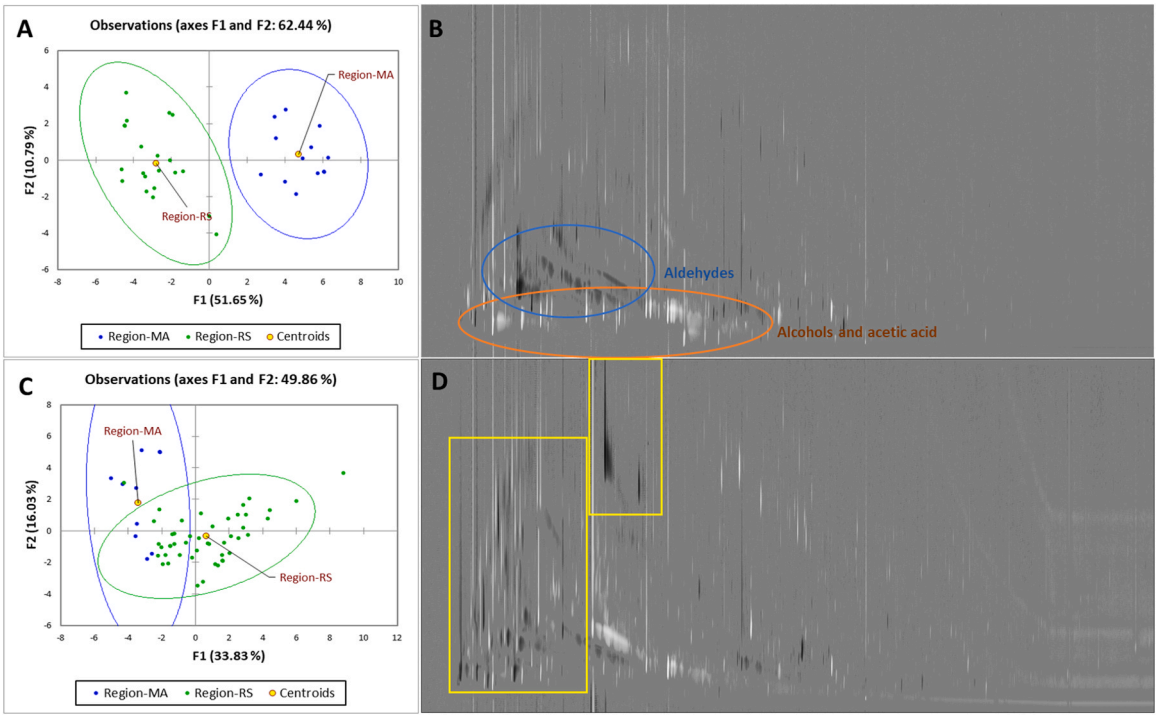

Fig. 1. A: PCA showing a natural clustering for Arbequina samples produced in 2021 and 2022 according to production region (PLS-DA followed by PCA). B: Comparison between cumulative images of Arbequina samples from RS (dark) and MA (bright) produced in 2021 and 2022. C: PCA showing a natural clustering for Koroneiki samples produced in 2021 and 2022 according to production region (PLS-DA followed by PCA). D: Comparison between cumulative images of Koroneiki samples from RS (dark) and MA (bright) produced in 2021 and 2022.

according to the production region, but the comparative overlayed visualization rendered as a grayscale fuzzy ratio indicated that samples from RS have higher relative amounts of most of the volatile compounds (darker part highlighted in yellow) than the samples from the MA region (brighter part). In Arbequina samples, 29 volatile compounds were important for discrimination according to region, while for Koroneiki samples this was for 28 analytes.

As in this research, other studies have demonstrated the role of volatile compounds in the geographic discrimination of olive oils (Stilo et al., 2021b). Lukić et al. (2019)) used target and untargeted volatile compounds for differentiation of VOOs produced from different cultivars in selected Croatian regions. The study concluded that this approach may have practical application in better understanding and classifying monovarietal VOOs according to production region and cultivar.

By using MHS-SPME followed by GC×GC-MS/FID, Stilo and collaborators identified discriminant chemical traits between Brazilian and Italian EVOOs. 1-Penten-3-one, (*Z*)-3-hexenal, (*E*)-2-hexenal, (*E*,*E*)-2,4-heptadienal, 1,8-cineole (eucalyptol), benzaldehyde, hexanal, and (*E*)-2-hexen-1-ol were quantified and identified as important compounds in this discrimination (Stilo et al., 2023). Brilhante et al. (2022) evaluated Brazilian EVOOs from Koroneiki cultivar from RS and MA and identified (*Z*)-3-hexenyl acetate as an important discriminant volatile compound in samples produced in MA and hexyl acetate in samples produced in RS.

3.3. Evaluation according to cultivar

After the comparison between regions, the next step was to compare cultivars. To perform the PCA, the samples were grouped according to regions (RS and MA) to try to discriminate them by cultivar (AR and KO). In Fig. 2A and B is shown the natural clustering according to cultivar for Arbequina and Koroneiki samples from MA and RS respectively. To perform these analyses, the samples coded as AR22_MA1 and KO22_MA1 were removed, and the reason why will be detailed later. Separating samples according to the production region, it was possible to observe good discrimination between the samples of different cultivars, mainly for those from the MA region (Fig. 2A). In MA samples, 31 volatile compounds were important for discrimination according to cultivar, while for RS samples this was for 22 analytes.

Cumulative images were also prepared to identify possible discriminants for EVOOs produced from each cultivar. In Fig. 3A is shown the comparative visualization rendered as a grayscale fuzzy ratio of a cumulative image of the Koroneiki samples from RS and MA and a cumulative image of the Arbequina samples from RS and MA, all produced in 2021 and 2022. Eight samples were used to create each Cumulative Class image. In Fig. 3B and C is shown the comparative visualization rendered as a grayscale fuzzy ratio of Koroneiki and Arbequina samples from MA and a cumulative image of the Koroneiki and Arbequina samples from RS, respectively.

It was possible to see in the three images that samples of the Arbequina cultivar (brighter part) have a higher relative amount of (*E*)-2-hexenal, while samples of the Koroneiki cultivar (darker part) have a higher amount of (*Z*)-3-hexenal; one non-identified compound (highlighted in yellow in the images) is also a common characteristic in the Koroneiki samples. In this case, the use of cumulative images can be an interesting approach to indicate distinctive characteristics between EVOOs produced from different cultivars.

The compounds observed in this study as cultivar markers were also reported in the literature (Lima et al., 2023). These authors found the (*Z*)-3-hexenal as the most abundant volatile compound in Koroneiki samples, while the (*E*)-2-hexenyl acetate was the most representative in Arbequina. In this work, for Arbequina samples, the compound that appeared in higher amounts was the (*E*)-2-hexenal, which can be converted in (*E*)-2-hexenyl acetate by alcohol acetyltransferase (AAT). Other research reported higher concentrations of C_6 compounds in Arbequina cultivar due to the high activity of hydroperoxide lyase in this cultivar (Sánchez-Ortiz et al., 2013).

3.4. The use of aroma blueprint to discriminate cultivars

Another approach used to discriminate samples according to cultivar was the determination of the aroma blueprint that characterizes EVOOs, using an Artificial Intelligence smelling machine concept (Nicolotti et al., 2019; Neugebauer et al., 2020). Fifteen key-aroma compounds and potent odorants were quantified by external calibration using an MHE-SPME-GC×GC-FID procedure and FID predicted RRFs based on combustion enthalpies (Neugebauer et al., 2020; Stilo et al., 2021b).

Using the quantified volatile compounds, the estimation of odor activity values (OAVs) was undertaken to provide a more accurate representation of the sensory impact of the most potent odorants on the overall aroma of EVOOs of each cultivar. In accordance with sensomic principles, an odorant is considered a key-aroma compound if it has an OAV exceeding 1 and if its presence in an aroma recombinant is relevant to properly distinguish the odor identity of a product (Dunkel et al., 2014).

In Fig. 4 is shown a spider diagram with aroma blueprint differences between Arbequina and Koroneiki samples. Results are presented as OAVs in $\log_{10}$ scale. Fourteen compounds make up the aroma blueprint

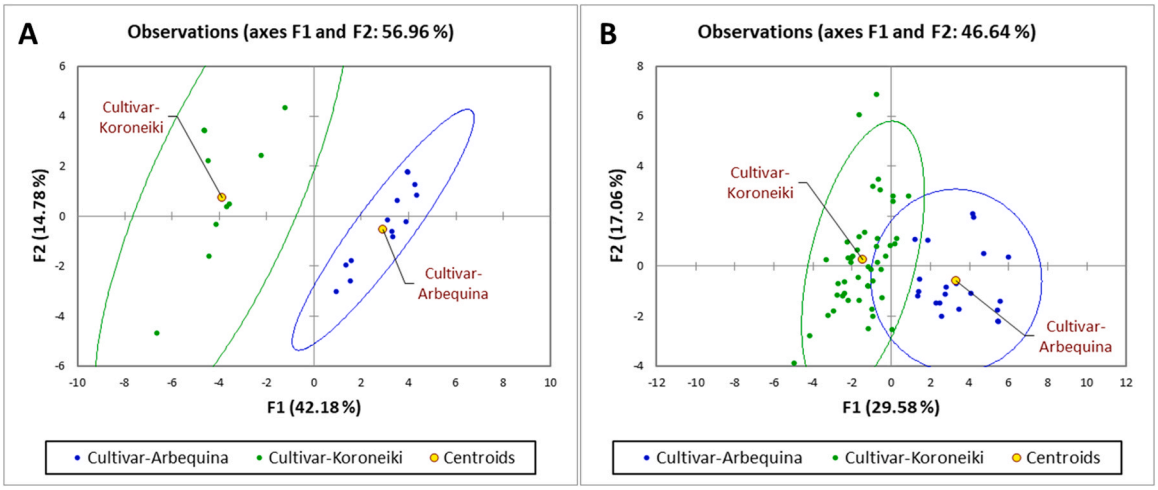

Fig. 2. A: PCA showing a natural clustering according to cultivar for Arbequina and Koroneiki samples from MA (PLS-DA followed by PCA). B: PCA showing a natural clustering according to cultivar for Arbequina and Koroneiki samples from RS (PLS-DA followed by PCA).

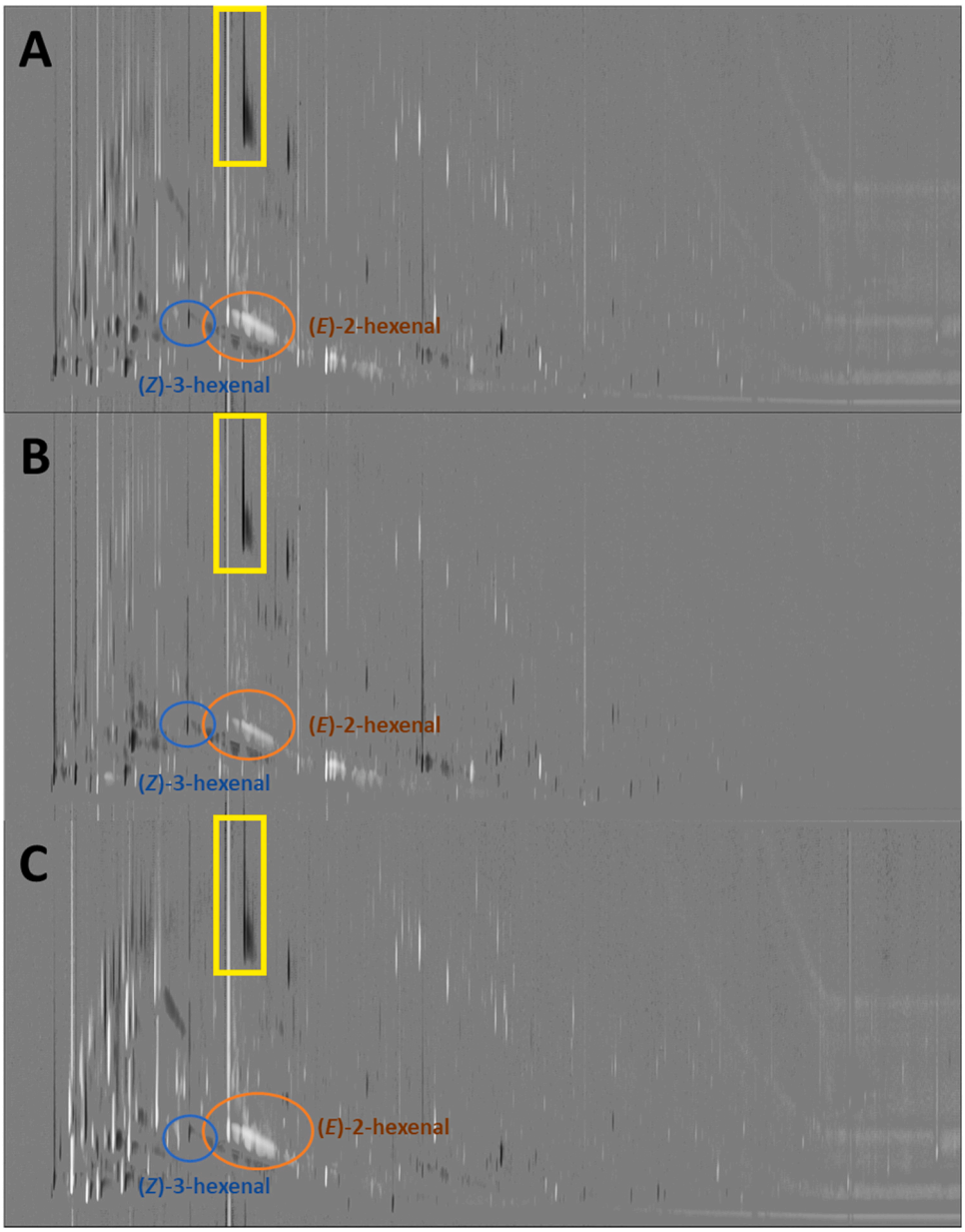

Fig. 3. A: Comparison between the cumulative image of 8 Koroneiki samples from RS and MA (dark) and the cumulative image of 8 Arbequina samples from RS and MA (bright). B: Comparison between the cumulative image of 4 Arbequina samples (bright) and the cumulative image of 4 Koroneiki samples (dark) from the MA region. C: Comparison between the cumulative image of 4 Arbequina samples (bright) and the cumulative image of 4 Koroneiki (dark) samples from RS. The cumulative images were created from samples produced in 2021 and 2022 crops.

of Brazilian EVOOs produced from Arbequina and Koroneiki cultivars: hexyl acetate (fruity), hexanal (green-apple, grass), 2-methylbutanal (malty), benzaldehyde (almond, burnt sugar), (*Z*)-3-hexenal (green, grassy), (*Z*)-3-hexen-1-ol (banana, fresh, grass), (*Z*)-2-penten-1-ol (green, almond), (*E*)-2-hexenal (bitter almond, green, fruity), (*E*,*E*)-2,4-heptadienal (fatty, green, oily), 1-penten-3-ol (pungent), (*Z*)-3-hexenyl acetate (green, banana-like), (*E*,*E*)-2,4-hexadienal (green), (*E*)-2-hexen-1-ol (green, grass), and 1-hexanol (fruity, banana, soft).

The most important compounds for the aroma blueprint discrimination of Arbequina samples were (*E*)-2-hexen-1-ol, with the descriptors of green and grass; (*E*)-2-hexenal, with the descriptors of bitter almond, green, and fruity; hexanal, with the descriptors of green-apple and grass; and 1-hexanol, with the descriptors of fruity, banana, and soft. In the case of Koroneiki samples, the main compounds that characterized this cultivar were (*Z*)-3-hexenal, which contributes with green and grassy odor; and (*Z*)-3-hexenyl acetate, with the descriptors of green and banana-like (Luna et al., 2006; Neugebauer et al., 2020). Not only compounds from the lipoxygenase pathway contribute to the aroma blueprint of Brazilian EVOOs and, with the exception of (*E*,*E*)-2,4-heptadienal, only those with positive odor descriptors were identified. This is in accordance with published data, as Stilo et al. (2023) found similar results in the comparison between Italian and Brazilian EVOOs blueprint. With the aroma blueprint, the objective comparison between samples was achieved and the results presented in the previous item were reinforced. The sensory peculiarities of each cultivar can be observed in the results presented.

3.5. GC×GC-MS/FID as a powerful tool to discriminate samples produced in different regions

Two samples were removed from the statistical analysis because the production regions were incorrectly stated on product labels

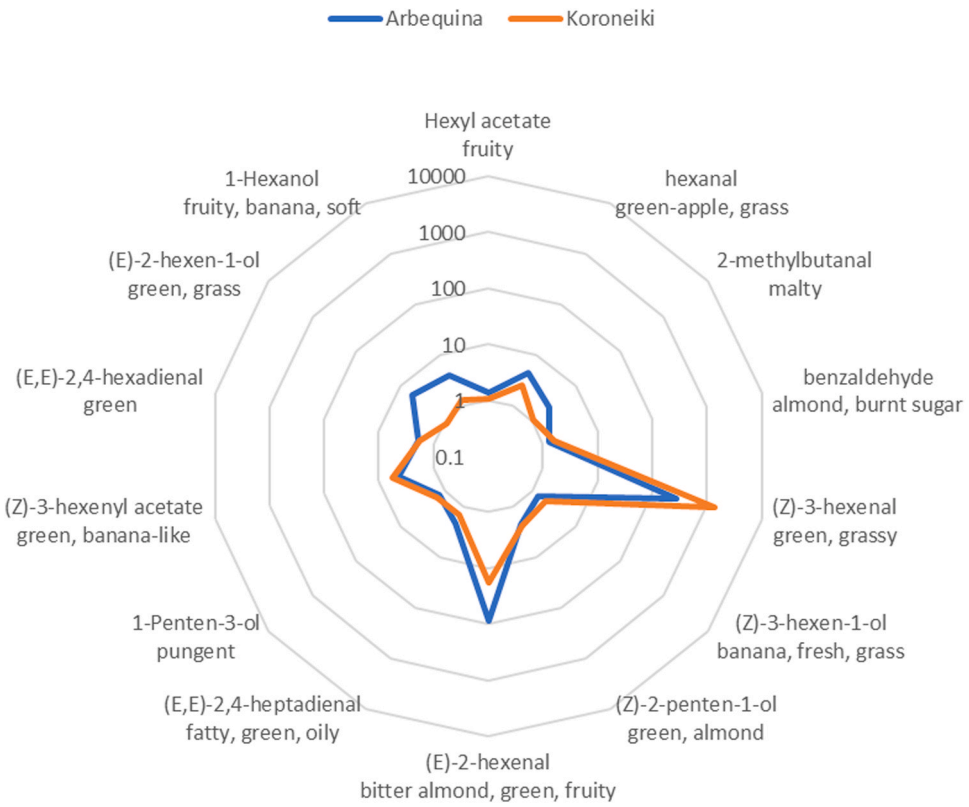

Fig. 4. The Spider diagram shows aroma blueprint differences between Arbequina and Koroneiki cultivars. Results are shown as Odor Activity Values (OAVs) in $\log_{10}$ scale.

(AR22_MA1 and KO22_MA1). The labels brought the allegation that the oils had been produced in the Mantiqueira region but, actually, they were from RS. This information was observed in the analyses presented in Fig. 5A and B and confirmed with the producers.

The Mantiqueira region comprises three states, Rio de Janeiro (RJ), Minas Gerais (MG), and São Paulo (SP), the samples analyzed in this research came from MG and SP. While EVOOs are produced in a flat region of the state of Rio Grande do Sul, those produced in Mantiqueira are grown in a region of mountains with different altitudes and sun incidence (Wrege et al., 2015). Knowing this, the Arbequina samples from Mantiqueira were divided by state of production to see if there was a difference in EVOOs produced in the same region but in different states. Fig. 5A shows the PCA performed for these samples. The same was done with the Koroneiki samples from Mantiqueira (Fig. 5B).

It was possible to observe that there is no separation by groups according to the state of production (SP x MG) for samples belonging to the same region (MA) but is possible to see that the samples coded AR22_MA1 and KO22_MA1 do not belong to the group of EVOOs from the MA region. After tracking them down using batch IDs, and without disclosing previously our results, it was confirmed by the respective producers that these two samples were from olives cultivated and processed in Rio Grande do Sul (RS region). It can be seen in Fig. 5C and D, in which these samples were placed together with those from the RS region, no cluster formation was observed.

The use of HS-SPME combined with GC×GC-MS/FID followed by the identification and quantification of volatile compounds present in the samples allowed to discriminate Brazilian EVOOs produced in different regions and from different cultivars. The analyses carried out with the AR22_MA1 and KO22_MA1 samples indicated the use of information encrypted in EVOOs volatilome as an efficient approach to identify cultivar and production region, which can be a tool to support claims for origin certification and food control agencies. To the best of our knowledge, this is the first reported case of mislabeling regarding geographical origin identified in Brazilian olive oils.

4. Conclusions

For the first time, 35 samples of the 2 main cultivars (Arbequina and Koroneiki) produced in the EVOOs producing regions in Brazil (Rio Grande do Sul and Serra da Mantiqueira) in two different crops (2021 and 2022) were analyzed to discriminate them according to production region and cultivar. The use of AI tools was also essential for data processing, another novelty for Brazilian EVOO samples.

MHS-SPME combined with GC×GC-MS/FID and quantification by external calibration and predicted RRF were a great tool in the quality assessment of EVOO samples. This technique, combined with the use of computer vision and the determination of EVOOs aroma blueprint, was also a valuable approach to indicate distinguishing characteristics between EVOOs produced in different regions (Rio Grande do Sul and Mantiqueira) and from different cultivars (Arbequina and Koroneiki).

The techniques used in this study can be applied not only for Brazilian EVOOs analysis, but for VOOs in general. As perspective, it is intended to create a database combining the data collected in this study with information on other olive oils produced in different regions and countries from different cultivars. This database can be used to identify the origin and cultivar of EVOOs, the second most frauded food in the world (Sudhakar et al., 2023). Indeed, during the method development, two mislabeled EVOOs, regarding their geographical origin, were identified amidst the samples analyzed. This is the first identification of mislabeled samples detected in Brazilian oils. Furthermore, this collection of data can be expanded to include information regarding adulteration and fraud profiles, and become a valuable tool for the Brazilian agencies of food control and law enforcement.

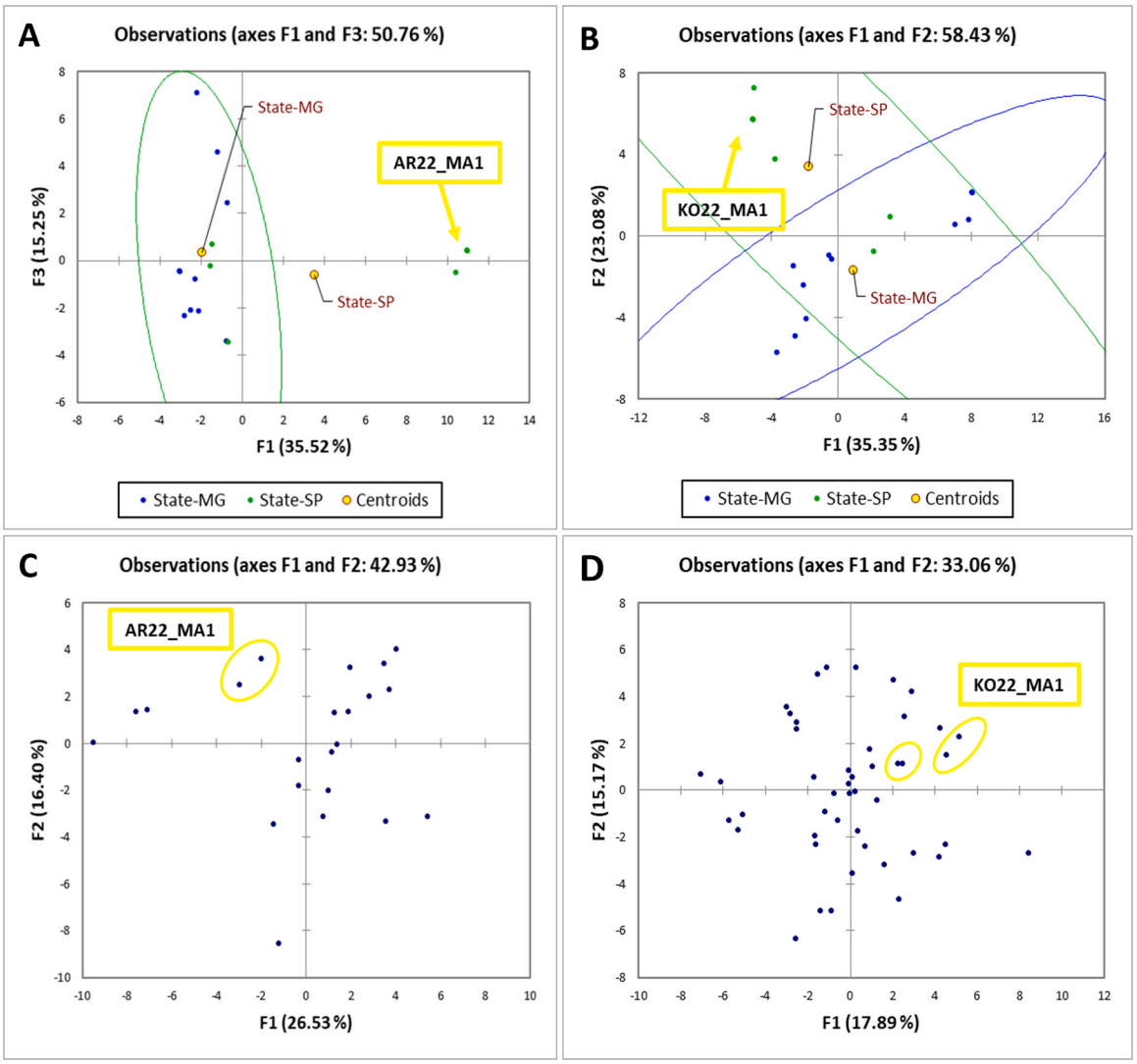

Fig. 5. A and B: PCA shows that there is no discrimination between EVOOs of the same region, only the samples AR22_MA1 and KO22_MA1, which belong to the RS region are separated from the others. C: PCA shows that there is no discrimination between the sample AR22_MA1 and the Arbequina samples from the RS region. D: PCA shows that there is no discrimination between the sample KO22_MA1 and the Koroneiki samples from the RS region.

CRediT authorship contribution statement

Simone Squara: Formal analysis, Data curation. **Chiara Cordero:** Writing – review & editing, Supervision, Resources, Methodology, Conceptualization. **Humberto R. Bizzo:** Writing – review & editing, Supervision, Funding acquisition, Conceptualization. **Andrea Caratti:** Formal analysis, Data curation. **Nathália S. Brilhante:** Writing – review & editing, Writing – original draft, Formal analysis, Data curation, Conceptualization.

Declaration of Competing Interest

The authors declare that they have no known competing financial interests or personal relationships that could have appeared to influence the work reported in this paper.

Acknowledgements

Funding: This work was supported by the Conselho Nacional de Desenvolvimento Científico e Tecnológico (CNPq) [311021/2021-2 and 406921/2022-9] and by the Coordenação de Aperfeiçoamento de Pessoal de Nível Superior (CAPES) [88887.695208/2022-00 and 88887.815139/2022-00], finance code 001.

Appendix A. Supporting information

Supplementary data associated with this article can be found in the online version at doi:10.1016/j.jfca.2024.106826.

Data availability

Data will be made available on request.

References

Adams, R., 2007. Identification of Essential Oil Components by Gas Chromatography-Mass Spectrometry, 4th ed.). Allured Publishing Corporation.

Babushok, V.I., Linstrom, P.J., Zenkevich, I.G., 2011. Retention indices for frequently reported compounds of plant essential oils. J. Phys. Chem. Ref. Data *40* (4), 043101. https://doi.org/10.1063/1.3653552.

Brasil. Diário Oficial da União. (2012). *Instrução Normativa no 1, de 30 de janeiro de 2012. Ministério Da Agricultura, Pecuária e Abastecimento - MAPA*, 1–6.

Brasil. Diário Oficial da União. (2018). *Instrução Normativa no 24, de 18 de junho de 2018. Ministério Da Agricultura, Pecuária e Abastecimento - MAPA*, 0(2), Edição: 117 | Seção: 1 | Página: 5.

Brazilian Agricultural Research Corporation – Embrapa. (2023). *Pesquisa atesta que Brasil produz azeite com padrão de qualidade internacional.* (https://www.embrapa.br/en/b

usca-de-noticias/-/noticia/82458918/pesquisa-atesta-que-brasil-produz-azeite-com-padrao-de-qualidade-internacional⟩.
Brereton, R.G., 2009. Chemometrics for Pattern Recognition. Chemometrics For Pattern Recognition. Wiley.
Brilhante, N.S., Faria-Machado, A.F., Antoniassi, R., Gama, P.E., Bizzo, H.R., 2022. Monitoring the profile of volatile compounds during the storage of extra virgin olive oils produced in Brazil from the koroneiki variety using the HS-SPME technique. Food Anal. Methods *15* (6), 1508–1520. https://doi.org/10.1007/s12161-021-02192-0.
Cachet, T., Brevard, H., Chaintreau, A., Demyttenaere, J., French, L., Gassenmeier, K., Joulain, D., Koenig, T., Leijs, H., Liddle, P., Loesing, G., Marchant, M., Merle, Ph, Saito, K., Schippa, C., Sekiya, F., Smith, T., 2016. IOFI recommended practice for the use of predicted relative-response factors for the rapid quantification of volatile flavouring compounds by GC-FID. Flavour Fragr. J. *31* (3), 191–194. https://doi.org/10.1002/ffj.3311.
Caratti, A., Squara, S., Bicchi, C., Liberto, E., Vincenti, M., Reichenbach, S.E., Tao, Q., Geschwender, D., Alladio, E., Cordero, C., 2024. Boosting comprehensive two-dimensional chromatography with artificial intelligence: application to food-omics. TrAC Trends Anal. Chem. *174*, 117669. https://doi.org/10.1016/j.trac.2024.117669.
Caratti, A., Squara, S., Bicchi, C., Tao, Q., Geschwender, D., Reichenbach, S.E., Ferrero, F., Borreani, G., Cordero, C., 2023. Augmented visualization by computer vision and chromatographic fingerprinting on comprehensive two-dimensional gas chromatographic patterns: unraveling diagnostic signatures in food volatilome. J. Chromatogr. A *1699*, 464010. https://doi.org/10.1016/j.chroma.2023.464010.
Caratti, A., Squara, S., Bicchi, C., Tao, Q., Geschwender, D., Reichenbach, S.E., Ferrero, F., Borreani, G., Cordero, C., 2023. Augmented visualization by computer vision and chromatographic fingerprinting on comprehensive two-dimensional gas chromatographic patterns: unraveling diagnostic signatures in food volatilome. J. Chromatogr. A *1699*, 464010. https://doi.org/10.1016/j.chroma.2023.464010.
Carvalho, A.G.A. de, Olmo-García, L., Gaspar, B.R.A., Carrasco-Pancorbo, A., Castelo-Branco, V.N., Torres, A.G., 2020. Evaluating quality parameters, the metabolic profile, and other typical features of selected commercial extra virgin olive oils from Brazil. Molecules *25* (18), 4193. https://doi.org/10.3390/molecules25184193.
Cordero, C., Liberto, E., Bicchi, C., Rubiolo, P., Reichenbach, S.E., Tian, X., Tao, Q., 2010. Targeted and non-targeted approaches for complex natural sample profiling by GCxGC-qMS. J. Chromatogr. Sci. *48* (4), 251–261. https://doi.org/10.1093/chromsci/48.4.251.
da Costa, J.R.O., Dal Bosco, S.M., Ramos, R.C. de S., Machado, I.C.K., Garavaglia, J., Villasclaras, S.S., 2020. Determination of volatile compounds responsible for sensory characteristics from Brazilian extra virgin olive oil using HS-SPME/GC-MS direct method. J. Food Sci. *85* (11), 3764–3775. https://doi.org/10.1111/1750-3841.15467.
Dunkel, A., Steinhaus, M., Kotthoff, M., Nowak, B., Krautwurst, D., Schieberle, P., Hofmann, T., 2014. Nature's chemical signatures in human olfaction: a foodborne perspective for future biotechnology. Angew. Chem. Int. Ed. *53* (28), 7124–7143. https://doi.org/10.1002/anie.201309508.
Filoda, P.F., Chaves, F.C., Hoffmann, J.F., Rombaldi, C.V., 2021. Olive oil: a review on the identity and quality of olive oils produced in Brazil. Rev. Bras. De. Frutic. *43* (3), 0–2. https://doi.org/10.1590/0100-29452021847.
Giardina, M., McCurry, J.D., Cardinael, P., Semard-Jousset, G., Cordero, C., Bicchi, C., 2018. Development and validation of a pneumatic model for the reversed-flow differential flow modulator for comprehensive two-dimensional gas chromatography. J. Chromatogr. A *1577*, 72–81. https://doi.org/10.1016/j.chroma.2018.09.022.
Granvogl, M., Schieberle, P., 2022. The sensomics approach: a useful tool to unravel the genuine aroma blueprint of foods and aroma changes during food processing. Compr. Anal. Chem. Vol. 96, 41–68. https://doi.org/10.1016/bs.coac.2021.10.002.
IOC. (2022). *IOC Olive Oil Dashboard*. ⟨https://www.internationaloliveoil.org/wp-content/uploads/2022/12/IOC-Olive-Oil-Dashboard-2.html#imports-1⟩.
Kalua, C.M., Allen, M.S., Bedgood, D.R., Bishop, A.G., Prenzler, P.D., Robards, K., 2007. Olive oil volatile compounds, flavour development and quality: a critical review. Food Chem. *100* (1), 273–286. https://doi.org/10.1016/j.foodchem.2005.09.059.
Kotsiou, K., Tasioula-Margari, M., 2015. Changes occurring in the volatile composition of Greek virgin olive oils during storage: oil variety influences stability. Eur. J. Lipid Sci. Technol. *117* (4), 514–522. https://doi.org/10.1002/ejlt.201400231.
Lima, A.F., da Silva Oliveira, W., de Oliveira Garcia, A., Vicente, E., Godoy, H.T., 2023. Identifying markers volatiles in Brazilian virgin oil by multiple headspace solid-phase microextraction, and chemometrics tools. Food Res. Int. *167*, 112697. https://doi.org/10.1016/j.foodres.2023.112697.
Lukić, I., Carlin, S., Horvat, I., Vrhovsek, U., 2019. Combined targeted and untargeted profiling of volatile aroma compounds with comprehensive two-dimensional gas chromatography for differentiation of virgin olive oils according to variety and geographical origin. Food Chem. *270* (March 2018)), 403–414. https://doi.org/10.1016/j.foodchem.2018.07.133.
Luna, G., Morales, M.T., Aparicio, R., 2006. Characterisation of 39 varietal virgin olive oils by their volatile compositions. Food Chem. *98* (2), 243–252. https://doi.org/10.1016/j.foodchem.2005.05.069.
Magagna, F., Cordero, C., Cagliero, C., Liberto, E., Rubiolo, P., Sgorbini, B., Bicchi, C., 2017. Black tea volatiles fingerprinting by comprehensive two-dimensional gas chromatography – mass spectrometry combined with high concentration capacity sample preparation techniques: Toward a fully automated sensomic assessment. Food Chem. *225*, 276–287. https://doi.org/10.1016/j.foodchem.2017.01.003.
Magagna, F., Guglielmetti, A., Liberto, E., Reichenbach, S.E., Allegrucci, E., Gobino, G., Bicchi, C., Cordero, C., 2017. Comprehensive chemical fingerprinting of high-quality cocoa at early stages of processing: effectiveness of combined untargeted and targeted approaches for classification and discrimination. J. Agric. Food Chem. *65* (30), 6329–6341. https://doi.org/10.1021/acs.jafc.7b02167.
Mariotti, M., Peri, C., 2014. The composition and nutritional properties of extra-virgin olive oil. Extra Virgin Olive Oil Handb. (2013), 21–34.
Morales, M.T., Rios, J.J., Aparicio, R., 1997. Changes in the volatile composition of virgin olive oil during oxidation: flavors and off-flavors. J. Agric. Food Chem. *45* (7), 2666–2673. https://doi.org/10.1021/jf960585+.
Neugebauer, A., Granvogl, M., Schieberle, P., 2020. Characterization of the key odorants in high-quality extra virgin olive oils and certified off-flavor oils to elucidate aroma compounds causing a rancid off-flavor. J. Agric. Food Chem. *68* (21), 5927–5937. https://doi.org/10.1021/acs.jafc.0c01674.
Nicolotti, L., Cordero, C., Cagliero, C., Liberto, E., Sgorbini, B., Rubiolo, P., Bicchi, C., 2013. Quantitative fingerprinting by headspace—two-dimensional comprehensive gas chromatography–mass spectrometry of solid matrices: some challenging aspects of the exhaustive assessment of food volatiles. Anal. Chim. Acta *798*, 115–125. https://doi.org/10.1016/j.aca.2013.08.052.
Nicolotti, L., Mall, V., Schieberle, P., 2019. Characterization of key aroma compounds in a commercial rum and an australian red wine by means of a new sensomics-based expert system (SEBES)—an approach to use artificial intelligence in determining food odor codes. J. Agric. Food Chem. *67* (14), 4011–4022. https://doi.org/10.1021/acs.jafc.9b00708.
Olias, J.M., Perez, A.G., Rios, J.J., Sanz, L.C., 1993. Aroma of virgin olive oil: Biogenesis of the "green" odor notes. J. Agric. Food Chem. *41* (12), 2368–2373. https://doi.org/10.1021/jf00036a029.
Reichenbach, S.E., Carr, P.W., Stoll, D.R., Tao, Q., 2009. Smart Templates for peak pattern matching with comprehensive two-dimensional liquid chromatography. J. Chromatogr. A *1216* (16), 3458–3466. https://doi.org/10.1016/j.chroma.2008.09.058.
Sánchez-Ortiz, A., Pérez, A.G., Sanz, C., 2013. Synthesis of aroma compounds of virgin olive oil: significance of the cleavage of polyunsaturated fatty acid hydroperoxides during the oil extraction process. Food Res. Int. *54* (2), 1972–1978. https://doi.org/10.1016/j.foodres.2013.03.045.
Schmarr, H.-G., Bernhardt, J., 2010. Profiling analysis of volatile compounds from fruits using comprehensive two-dimensional gas chromatography and image processing techniques. J. Chromatogr. A *1217* (4), 565–574. https://doi.org/10.1016/j.chroma.2009.11.063.
Schmarr, H.-G., Bernhardt, J., Fischer, U., Stephan, A., Müller, P., Durner, D., 2010. Two-dimensional gas chromatographic profiling as a tool for a rapid screening of the changes in volatile composition occurring due to microoxygenation of red wines. Anal. Chim. Acta *672* (1–2), 114–123. https://doi.org/10.1016/j.aca.2010.05.002.
Stilo, F., Jiménez-Carvelo, A.M., Liberto, E., Bicchi, C., Reichenbach, S.E., Cuadros-Rodríguez, L., Cordero, C., 2021. Chromatographic fingerprinting enables effective discrimination and identitation of high-quality italian extra-virgin olive oils. J. Agric. Food Chem. *69* (31), 8874–8889. https://doi.org/10.1021/acs.jafc.1c02981.
Stilo, F., Bicchi, C., Jimenez-Carvelo, A.M., Cuadros-Rodriguez, L., Reichenbach, S.E., Cordero, C., 2021a. Chromatographic fingerprinting by comprehensive two-dimensional chromatography: fundamentals and tools. TrAC Trends Anal. Chem. 134, 116133. https://doi.org/10.1016/j.trac.2020.116133.
Stilo, F., SeguraBorrego, M. del P., Bicchi, C., Battaglino, S., CallejónFernandez, R.M., Morales, M.L., Reichenbach, S.E., Mccurry, J., Peroni, D., Cordero, C., 2021b. Delineating the extra-virgin olive oil aroma blueprint by multiple headspace solid phase microextraction and differential-flow modulated comprehensive two-dimensional gas chromatography. J. Chromatogr. A 1650, 462232. https://doi.org/10.1016/j.chroma.2021.462232.
Stilo, F., Liberto, E., Spigolon, N., Genova, G., Rosso, G., Fontana, M., Reichenbach, S.E., Bicchi, C., Cordero, C., 2021c. An effective chromatographic fingerprinting workflow based on comprehensive two-dimensional gas chromatography – mass spectrometry to establish volatiles patterns discriminative of spoiled hazelnuts (*Corylus avellana* L.). Food Chem. 340, 128135. https://doi.org/10.1016/j.foodchem.2020.128135.
Stilo, F., Alladio, E., Squara, S., Bicchi, C., Vincenti, M., Reichenbach, S.E., Cordero, C., Bizzo, H.R., 2023. Delineating unique and discriminant chemical traits in Brazilian and Italian extra-virgin olive oils by quantitative 2D-fingerprinting and pattern recognition algorithms. J. Food Compos. Anal. *115*, 104899. https://doi.org/10.1016/j.jfca.2022.104899.
Sudhakar, A., Chakraborty, S.K., Mahanti, N.K., Varghese, C., 2023. Advanced techniques in edible oil authentication: a systematic review and critical analysis. Crit. Rev. Food Sci. Nutr. *63* (7), 873–901. https://doi.org/10.1080/10408398.2021.1956424.
The European Commission. (2016). Commission Delegated Regulation (EU) 2016/2095 amending Regulation (EEC) No 2568/91 on the characteristics of olive oil and olive-residue oil and on the relevant methods of analysis. *Official Journal of the European Union, L326*(September 2016), 1–6. ⟨https://eur-lex.europa.eu/legal-content/EN/TXT/PDF/?uri=CELEX:32016R2095&from=PT⟩.
Uekane, T.M., Nicolotti, L., Griglione, A., Bizzo, H.R., Rubiolo, P., Bicchi, C., Rocha-Leão, M.H.M., Rezende, C.M., 2017. Studies on the volatile fraction composition of three native Amazonian-Brazilian fruits: Murici (Byrsonima crassifolia L., Malpighiaceae), bacuri (Platonia insignis M., Clusiaceae), and sapodilla (Manilkara sapota L., Sapotaceae). Food Chem. *219*, 13–22. https://doi.org/10.1016/j.foodchem.2016.09.098.

van Den Dool, H., Dec. Kratz, P., 1963. A generalization of the retention index system including linear temperature programmed gas—liquid partition chromatography. J. Chromatogr. A *11*, 463–471. https://doi.org/10.1016/S0021-9673(01)80947-X.

Wrege, M.S., Coutinho, E.F., Pantano, A.P., Oliveira, R., 2015. Distribuição potencial de oliveiras no brasil e no mundo. Rev. Bras. De. Frutic. *37* (3), 656–666. https://doi.org/10.1590/0100-2945-174/14.

Zago, L., Squeo, G., Bertoncini, E.I., Difonzo, G., Caponio, F., 2019. Chemical and sensory characterization of Brazilian virgin olive oils. Food Res. Int. *126*, 108588. https://doi.org/10.1016/j.foodres.2019.108588.